

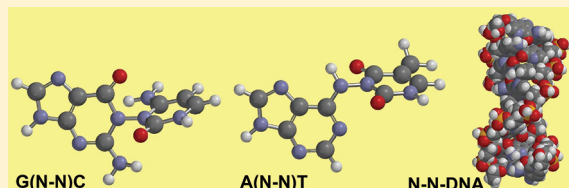
# Formation of N–N Cross-Links in DNA by Reaction of Radiation-Produced DNA Base Pair Diradicals: A DFT Study

Venkata Pottiboyina, Anil Kumar, and Michael D. Sevilla\*

Department of Chemistry, Oakland University, Rochester, Michigan 48309, United States

Supporting Information

**ABSTRACT:** This study employs DFT (density functional theory) to investigate the formation of hydrazine-like (N–N) cross-linked structures between DNA base pair diradicals that are likely to result from the interaction of high linear energy transfer (LET) radiation, such as ion-beam radiation, with DNA. In our calculations, we generated the guanine (G), cytosine (C), adenine (A), and thymine (T) radicals by removing one hydrogen atom from an N–H bond involved in the normal base pairing. The radical species formed are those that naturally result from one-electron oxidation of the bases followed by deprotonation. N–N cross-links between G and C or A and T diradicals were studied using the BHandHLYP, B3LYP, M06, and M06-2X density functionals and 6-31G\* basis set. From a comparison to several test cases performed with the G3B3 method, which gives thermodynamically reliable values, we found that calculations employing the BHandHLYP/6-31G\* method predict the best estimates of bonding energies for hydrazine-like structures. Our study shows that the N–N cross-link formed between guanine radical and a neutral cytosine is endothermic in nature but can form metastable structures. However, the reactions between two DNA base radicals (diradical) to form several N–N cross-linked structures are found to be highly exothermic in nature. The N–N cross-links formed between various G–C, G–G, and C–C diradicals have binding energies in the range of ca. –54 to –68, –41 to –47, and –67 to –75 kcal/mol, respectively, whereas A–T, A–A, and T–T have binding energies of –80, –60, and –98 kcal/mol, respectively. In all purine–pyrimidine N–N cross-linked structures, the highest occupied molecular orbital (HOMO) is found to be localized on the purine moiety and the lowest unoccupied molecular orbital (LUMO) is on the pyrimidine moiety.



## INTRODUCTION

Exposure of DNA to high-energy radiation results in ionization of each portion of DNA including the bases and the sugar–phosphate backbone that initially yield anion and cation radical species, which on proton-transfer reactions often become neutral radicals.<sup>1</sup> Ionizing radiation produces ionizations with stochastic spacings in which a single event yields two proximate ionizations a significant fraction of the time. For example, in water a 1 MeV electron will deposit on average about 50 eV and cause 1.8 ionizations per event (spur).<sup>2</sup> In DNA the energy loss spectrum of the electron is found to be near that of water.<sup>3</sup> Thus, multiple proximate ionizations are expected from such low linear energy transfer (LET) radiation, and radicals should be formed in close proximity (within 2 nm). For high-LET radiation such as  $\alpha$  particles or heavier ion beams a densely ionized track is formed in which near neighbor molecules have a much higher probability of ionization with associated radical formation.<sup>4</sup> The proximate radicals produced in these tracks have a high probability of recombination to form new molecular species with unique structures.

It is well-known that DNA constituents and proteins are highly susceptible to attack by reactive oxygen species (ROS) which produce one-electron-oxidized radical species and subsequent DNA damage such as cross-links and strand breaks. A variety of cross-links have been identified including, protein–protein, protein–DNA, or cross-links between and within DNA strands.<sup>5</sup> The experimental literature is rich with reports of

a variety of base-to-base<sup>5b,c</sup> and intrastrand sugar–base<sup>5c</sup> DNA cross-links, e.g., thymine–thymine cyclobutane dimers produced under UV irradiation<sup>5b</sup> and sugar–C<sub>5'</sub>–guanine/adenine–C<sub>8</sub> cross-links.<sup>5c</sup> Single radical-induced interstrand cross-link formation have also been reported, such as cross-links formed by 5-(2'-deoxyuridinyl)methyl radical attack on deoxyadenosine (dA) and 2'-deoxycytidine-5-yl radical reaction with dA and deoxyguanosine (dG).<sup>5c,6a</sup> Several guanine-to-guanine cross-links such as dG(N2)–(C2)dG and dG(N1)–(C2)dG have been found experimentally and studied theoretically.<sup>6b–i</sup> A cross-linked GC structure bridged by an alkyl link between N1 of guanine and N3 of cytosine has also been identified.<sup>6j,k</sup> Using the B3LYP method, the radiation-induced formation of interstrand cross-links (5'-AT-3' and 5'-TA-3') between the C8 position in adenine and the methyl group in thymine were studied by Xerri et al.<sup>6l</sup> We note that N–N cross links between phenylnitrenium ion and N-7 on guanine derivatives has been reported.<sup>6m</sup>

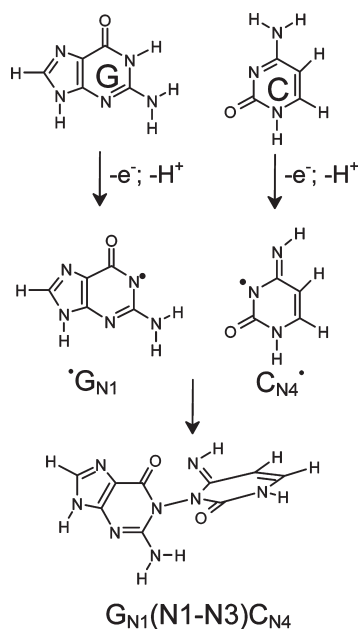
Although it is expected that biradical formation in DNA base pairs should be formed by ionizing radiation with increasing probability as the LET of the radiation increases, few works have described such events.<sup>7</sup> However, in irradiated crystalline thymine at 77 K, a strong radical pair EPR (electron paramagnetic

Received: August 16, 2011

Revised: October 28, 2011

Published: November 03, 2011

**Scheme 1. Schematic Diagram Showing the Formation of N–N Cross-Linked Structures, e.g.,  $G_{N1}(N1-N3)C_{N4}$ , Due to Reaction between  $\cdot G_{N1}$  and  $C_{N4}\cdot$ <sup>a</sup>**



<sup>a</sup> Note that  $G_{N1}(N1-N3)C_{N4}$  indicates a bond between N1 and N3 on G and C, after one-electron oxidation and proton loss from the N1 and N4 positions of G and C, respectively. For numbering see the figure in Table 1.

resonance) signal is found from the radical–radical interaction of the two major radical species formed by hydrogen atom loss and hydrogen atom gain, i.e.,  $\text{Thy}(\text{Me} - \text{H})\cdot$  and  $\text{Thy}(\text{C6} + \text{H})\cdot$ , respectively.<sup>8</sup> Using EPR, Peoples et al.<sup>9</sup> have investigated the possible diradical formation in calf thymus DNA films which were X-irradiated at 4 K. Since the DNA samples were amorphous, they did not observe diradical signals in the EPR spectra and were only able to set an upper limit to their formation. Nevertheless, radical–radical reactions have been rarely invoked for DNA cross-link formation since most have been expected to be induced by more numerous single-radical events. However, we note that radical–radical reactions must be considered likely given the spatial distribution of ionizations induced by high-energy radiations. In one-electron-oxidized DNA, guanine cation radical has been shown by ESR (electron spin resonance) spectroscopy to deprotonate at both N1 and N2-sites in the (G–C) base pair.<sup>10</sup> It would be expected that such species would be formed simultaneously with a base-paired one-electron-oxidized cytosine and could undergo radical–radical reactions.

Quantum chemical calculations, using reliable methods such as DFT (density functional theory), can provide thermodynamic and structural properties for radical–radical reactions. In recent years, such efforts have been made to understand the structures and stabilities of radicals formed on DNA bases as well as guanine–cytosine (G–C) and adenine–uracil base pairs by hydrogen abstraction from different sites using DFT by Schaefer and co-workers.<sup>11</sup> Very recently, the diradicals of guanine–cytosine base pair were studied by Seal et al.<sup>12</sup> using the spin-polarized Moller–Plesset perturbation (MP2) and spin-flip broken symmetry (SF-BS-DFT) methods. In their study, they removed two non-hydrogen-bonding hydrogen atoms simultaneously from

guanine–cytosine base pair to generate diradicals and studied their magnetic properties but no radical–radical reactions were investigated.

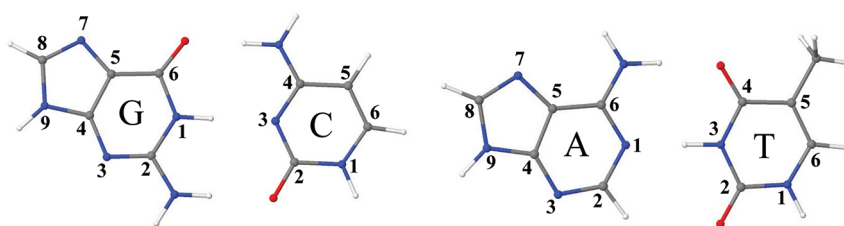
In this study, we considered the N–N cross-linking of G–C and A–T base pairs from radical and diradical precursors. The potential energy surface, the structure, and binding properties of the newly formed cross-link structures were studied using DFT. In addition to G–C and A–T diradicals, we also considered the N–N cross-link formation in homopurines and homopyrimidines, viz., A–A, G–G, C–C, and T–T. The T–T cross-link has been found to be the most stable with a calculated binding energy of  $-98$  kcal/mol. To our knowledge, no theoretical study to date considers such hydrazine-like covalent cross-links in DNA base pairs that are predicted in this work to be produced in doubly oxidized DNA base pairs.

## METHOD OF CALCULATIONS

In the present study, we considered G–C and A–T base pair single radical and diradical reactions that result in hydrazine-like N–N covalent bond formation. From the base pairs under consideration, we generated a guanine base radical by removing a hydrogen atom from the N–H bond at the base pairing site and studied reactions with its nonradical complementary base cytosine to form an N–N cross-link between them. Second, we removed an N–H hydrogen atom from each of the two bases forming the base pair from their N–H bond simultaneously to form diradicals and studied their reaction to form an N–N cross-link between them. A generalized labeling is used to represent the structure resulting from reaction between two radicals, see Scheme 1. For example, the label  $G_{N1}(N1-N3)C_{N4}$  means that hydrogen atoms are abstracted from the N1–H bond of guanine and N4–H bond of cytosine forming radicals  $\cdot G_{N1}$  and  $C_{N4}\cdot$  that react to make an N1–N3 bond between them, see Scheme 1. The binding energy of the various N–N cross-links is calculated using the BHandHLYP, B3LYP, M06, and M06-2X methods and 6-31G\* basis set. In Table 1, we present the binding energy calculated by the BHandHLYP/6-31G\* method because this functional is found to be more suitable for NN bonding than the other functionals; see the discussion in the next section. However, the data generated by B3LYP, M06, and M06-2X methods are presented in the Supporting Information as Table S1. All the calculations were done using the Gaussian 09 suite of programs.<sup>13</sup> Molecular orbitals and spin density distribution diagrams were plotted using the GaussView molecular modeling software.<sup>14</sup> The JMOL program was used to draw the molecular structures.<sup>15</sup>

## RESULTS AND DISCUSSION

**I. Suitability of the Functional.** From several years, the applicability of the DFT has been found very successful in describing molecular structures and their various properties. Because of its moderate computational cost (comparable to Hartree–Fock calculation), accuracy, and applicability to large molecules (ca. 1000 atoms), it has now become the first choice for the computational chemist.<sup>16</sup> Even though increasingly employed as a useful methodology, DFT is found to suffer from the self-interaction error (SIE) and can underestimate the bond dissociation energies of radicals, e.g.,  $\text{H}_2\cdot^+$ .<sup>17</sup> New functionals have been developed that minimizes the SIE by increasing the Hartree–Fock exchange contribution in the functional or by the

**Table 1.** BHandHLYP/6-31G\*-Calculated Binding Energy ( $\Delta E$ , kcal/mol) of Proposed Interstrand Cross-Link Structures Formed between G, C, A, and T Radicals

structure no.	species A	species B	cross-linked species <sup>a</sup>	$\Delta E^{b,c}$ (kcal/mol)
GC radical	G radical <sup>d</sup>	C molecule <sup>e</sup>	G(X–Y)C radical <sup>a</sup>	
1	<sup>•</sup> G <sub>N1</sub>	C	G <sub>N1</sub> (N1–N3)C <sup>•</sup>	9.96
2	<sup>•</sup> G <sub>N2</sub>	C	G <sub>N2</sub> (N2–N3)C <sup>•</sup>	12.11
GC diradical	G radical	C radical	G(X–Y)C molecule <sup>a</sup>	
3	<sup>•</sup> G <sub>N1</sub>	C <sup>•+</sup>	G <sub>N1</sub> (N1–N3)C <sup>+</sup>	–67.52
4	<sup>•</sup> G <sub>N2</sub>	C <sup>•+</sup>	G <sub>N2</sub> (N2–N3)C <sup>+</sup>	–59.61
5	<sup>•</sup> G <sub>N1</sub>	<sup>•</sup> C <sub>N4</sub>	G <sub>N1</sub> (N1–N3)C <sub>N4</sub>	–56.26
6	<sup>•</sup> G <sub>N1</sub>	<sup>•</sup> C <sub>N4</sub>	G <sub>N1</sub> (N1–N4)C <sub>N4</sub>	–64.70
7	<sup>•</sup> G <sub>N2</sub>	<sup>•</sup> C <sub>N4</sub>	G <sub>N2</sub> (N2–N3)C <sub>N4</sub>	–54.36
8	<sup>•</sup> G <sub>N2</sub>	<sup>•</sup> C <sub>N4</sub>	G <sub>N2</sub> (N2–N4)C <sub>N4</sub>	–58.55
AT diradical	A radical	T radical	A(X–Y)T molecule <sup>a</sup>	
9	<sup>•</sup> A <sub>N6</sub>	<sup>•</sup> T <sub>N3</sub>	A <sub>N6</sub> (N6–N3)T <sub>N3</sub>	–79.52
GG diradical	G radical	G radical	G(X–Y)G molecule <sup>a</sup>	
10	<sup>•</sup> G <sub>N2</sub>	<sup>•</sup> G <sub>N2</sub>	G <sub>N2</sub> (N2–N2)G <sub>N2</sub>	–40.49
11	<sup>•</sup> G <sub>N2</sub>	<sup>•</sup> G <sub>N1</sub>	G <sub>N2</sub> (N2–N1)G <sub>N1</sub>	–45.32
12	<sup>•</sup> G <sub>N1</sub>	<sup>•</sup> G <sub>N1</sub>	G <sub>N1</sub> (N1–N1)G <sub>N1</sub>	–47.32
AA diradical	A radical	A radical	A(X–Y)A molecule <sup>a</sup>	
13	<sup>•</sup> A <sub>N6</sub>	<sup>•</sup> A <sub>N6</sub>	A <sub>N6</sub> (N6–N6)A <sub>N6</sub>	–60.43
CC diradical	C radical	C radical	C(X–Y)C molecule <sup>a</sup>	
14	<sup>•</sup> C <sub>N4</sub>	<sup>•</sup> C <sub>N4</sub>	C <sub>N4</sub> (N4–N4)C <sub>N4</sub>	–75.25
15	<sup>•</sup> C <sub>N4</sub>	<sup>•</sup> C <sub>N4</sub>	C <sub>N4</sub> (N3–N3)C <sub>N4</sub>	–66.94
16	<sup>•</sup> C <sub>N4</sub>	<sup>•</sup> C <sub>N4</sub>	C <sub>N4</sub> (N3–N4)C <sub>N4</sub>	–71.64
TT diradical	T radical	T radical	T(X–Y)T molecule <sup>a</sup>	
17	<sup>•</sup> T <sub>N3</sub>	<sup>•</sup> T <sub>N3</sub>	T <sub>N3</sub> (N3–N3)T <sub>N3</sub>	–97.51


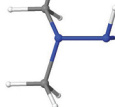
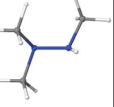
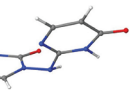
<sup>a</sup> Bonding between the X nitrogen atom of the guanine radical and the Y nitrogen atom of the cytosine molecule, cation radical, or neutral radicals/molecule as indicated. <sup>b</sup> See the Supporting Information for the structure. <sup>c</sup> Binding energy = TE of cross-link species – (TE of species A + TE of species B). TE = total energy without zero-point energy corrections. <sup>d</sup> Site of hydrogen atom abstraction in guanine is given as a subscript. <sup>e</sup> C = cytosine, C<sup>•+</sup> = cytosine cation radical. C<sub>N4</sub><sup>•</sup> indicates the hydrogen atom abstraction from N4 in cytosine.

use of empirical correction schemes. In the present study we selected B3LYP, BHandHLYP, M06, M06-2X, W97X, and W97X-D functionals to test their suitability for the structures under consideration. For the test cases, we considered hydrazine, di- and trimethyl hydrazine, and a model compound resembling the base pair structure shown in Table 2. We used hydrazine and substituted hydrazine structures as test cases because in the present study all the structures have the N–N hydrazine-like cross-link and for hydrazines experimental binding energies are available or can be accurately calculated using the G3B3 method.<sup>18</sup> Hydrazine and di- and trimethyl hydrazines were also previously studied using different density functionals and ab initio MP2, MP4, and QCISD methods, and in these studies the calculated binding energies were compared with the available experimental data.<sup>19</sup> Thus, in addition to the earlier studies<sup>19</sup> we are supplementing the data generated by the use of M06, M06-

2X, W97X, and W97X-D in Table 2 to test the suitability of a functional for this class of molecules. From Table 2, we found that among all the functionals, the calculated binding energies by the BHandHLYP method is very close to the experimental data and has the smallest average deviation with G3B3 values, see Table 2. In the text, we present our data using the BHandHLYP/6-31G\* method; however, the data generated by B3LYP, M06, and M06-2X are presented in Table S1 in the Supporting Information.

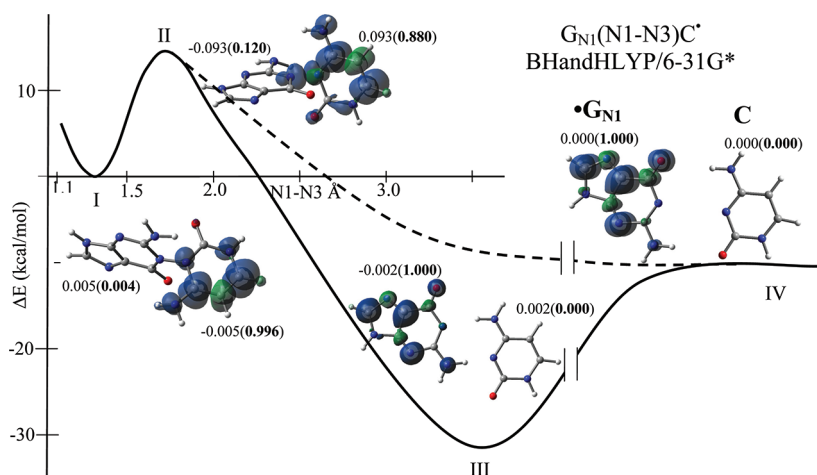
**II. Radical Cross-Link Formation between Guanine Radical and Cytosine.** From theory and experiment it is well-established that among all the DNA bases (A, T, G, and C) guanine has the smallest ionization potential, and thus, it is the primary site for oxidation (electron loss center) in DNA.<sup>1</sup> The one-electron-oxidized guanine (G<sup>•+</sup>) is acidic and has the pK<sub>a</sub> = 3.9.<sup>20</sup> From ESR and pulse radiolysis experiments it is found that the G<sup>•+</sup>

**Table 2.** Binding Energy ( $\Delta E$ , kcal/mol) of Hydrazine, Di- and Tri-methyl Hydrazines, and a Model Compound Calculated Using Different Methods along with Experimental Values<sup>j</sup>

Method					
	ΔE (kcal/mol)				
G3B3	-63.72 (65.8± 2) <sup>a</sup>	-61.52 (59.0±2) <sup>a</sup>	-60.11	-51.51 <sup>b</sup>	Avg. Dev. <sup>c</sup>
BHandHLYP <sup>d,h</sup>	-64.19	-58.50	-54.39	-55.37	1.10
B3LYP <sup>d,h</sup>	-69.78	-62.85	-57.67	-57.16	-2.65
BLYP <sup>d,h</sup>	-70.15	-62.51	-56.55	-53.75	-1.53
M06-2X <sup>d,i</sup>	-77.68	-73.22	-69.84	-73.03	-14.23
M06 <sup>d,i</sup>	-75.31	-69.15	-64.81	-65.54	-9.49
WB97XD <sup>d,i</sup>	-75.44	-69.25	-65.04	-67.26	-10.03
WB97X <sup>d,i</sup>	-76.80	-69.44	-65.09	-67.26	-10.43
MP2 <sup>d,e</sup>	-63.9	-	-	-	
MP4 <sup>f</sup>	-59.2	-	-	-	
QCISD	-58.9 <sup>g</sup> -61.7 <sup>g</sup>	-	-	-	

<sup>a</sup> Experimental values in parentheses from ref 19b. <sup>b</sup> Hydrazine bonding between two pyrimidine rings. <sup>c</sup> Calculated as deviations from G3B3 values.

<sup>d</sup> Calculated using 6-31G\* basis set without zero-point energy (ZPE) correction. <sup>e</sup> MP2 calculation includes ZPE correction, ref 19a. <sup>f</sup> Calculated using 6-311++G\*\* basis set, and includes ZPE correction, ref 19a. <sup>g</sup> Calculated using 6-311++G(2df, p) basis set, and includes ZPE correction, ref 19a. <sup>h</sup> From ref 19b. <sup>i</sup> Present study. <sup>j</sup> Binding energies were calculated using the radical–radical reaction  $R1R2N^{\bullet} + R3R4N^{\bullet} \rightarrow (R1, R2)N-N(R3, R4)$  (where R1, R2, R3, and R4 are substituents).



**Figure 1.** BHandHLYP/6-31G\*-calculated potential energy surface (kcal/mol) for the formation of N–N cross-linked GC base pair ( $G_{N1}(N1-N3)C^{\bullet}$ ) on reaction between  $\bullet G_{N1}$  and neutral cytosine. The spin density distribution on the molecule is also shown. The lowest energy structure is the hydrogen-bonded structure. At the right the initial separate species are shown. The net charge and spin (in parentheses in bold) residing in each moiety are also shown. The charge and spin density distribution at each atom of species numbered as I, II, III, and IV are given in Table S2 in the Supporting Information.

deprotonates either from its N1 or N2 site to form neutral radicals  $\bullet G_{N1}$  and  $\bullet G_{N2}$ , respectively.<sup>10,20,21</sup> The transiently formed  $\bullet G_{N1}$  and  $\bullet G_{N2}$  in DNA disrupt the normal hydrogen-bonding pattern with its complementary hydrogen-bonded cytosine and results in the formation of slipped hydrogen-bonded but still base-paired structure.<sup>10,11b,22</sup> In this work, we initially investigated the reaction of  $\bullet G_{N1}$  and  $\bullet G_{N2}$  with the neutral cytosine base to form the radicals  $G_{N1}(N1-N3)C^{\bullet}$  and  $G_{N2}(N2-N3)C^{\bullet}$ , respectively, see Table 1. The BHandHLYP/6-31G\*-calculated potential energy surface (PES) of the reaction between  $\bullet G_{N1}$  and cytosine resulting in  $G_{N1}(N1-N3)C^{\bullet}$  is shown in Figure 1 while the corresponding PES for the formation of  $G_{N2}(N2-N3)C^{\bullet}$  is shown in the Supporting Information as Figure S1.

In Figure 1, the nature of the spin density distribution at some chosen points on the PES is also shown. From Figure 1, it is evident that the reaction of  $\bullet G_{N1}$  with cytosine proceeds on two surfaces with the formation of two types of structures: (i) The slipped form hydrogen-bonded planar structure in which the guanine and cytosine bases are held together by the two hydrogen bonds, see Figure 1. This structure has the binding energy of  $-30$  kcal/mol with respect to the isolated  $\bullet G_{N1}$  and cytosine. The formation of this structure in a DNA oligomer was previously proposed by DFT calculations.<sup>10,11a,22</sup> (ii) N1–N3 cross-link formation  $G_{N1}(N1-N3)C^{\bullet}$ . In this structure guanine and cytosine rings are oriented by ca.  $90^\circ$ , and the N1–N3 bond is formed. This structure lies about 10 kcal/mol above the



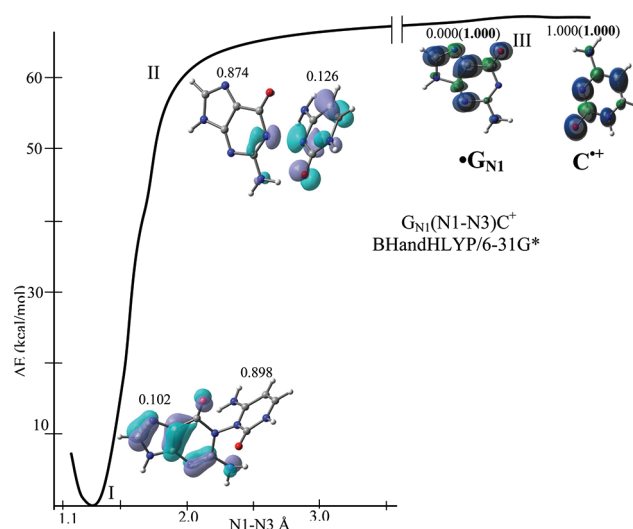
isolated  $\cdot G_{N1}$  and cytosine, and from the PES (Figure 1) it is evident that it is metastable with an activation barrier of ca. 15 kcal/mol for its dissociation. From the nature of the spin density distributions in these two structures, we found that, in the hydrogen-bonded GC base-paired structure, spin densities are localized on guanine only (as is well-known), whereas in the  $G_{N1}(N1-N3)C^+$  cross-linked species spin densities are completely transferred to cytosine with a spin distribution much like the cytosine one-electron adduct, see Figure 1. Clearly on N1–N3 bonding, a  $\sigma\pi^*$  three-electron bond is formed with a strong  $\sigma$ -bond between two nitrogens with one electron forced into the extended  $\pi^*$  system of cytosine in an antibonding molecular orbital (lowest unoccupied molecular orbital, LUMO).

The  $G_{N2}(N2-N3)C^+$  cross-link species lies ca. 12 kcal/mol above the separated  $\cdot G_{N2}$  and cytosine, see Figure S1 in the Supporting Information. However, it also shows a local minimum with a barrier of ca. 19 kcal/mol toward dissociation. From the PES (Supporting Information Figure S1), we see again that the hydrogen-bonding structure is substantially more stable (20 kcal/mol) than the  $G_{N2}(N2-N3)C^+$  cross-link as found for  $G_{N1}(N1-N3)C^+$ .

**III. Cross-Link Formation between Guanine Radical and Cytosine Radical (GC Diradical).** There are six possible structures that form N–N cross-links by reaction between a guanine radical and a cytosine radical, namely,  $G_{N1}(N1-N3)C^+$ ,  $G_{N2}(N2-N3)C^+$ ,  $G_{N1}(N1-N3)C_{N4}$ ,  $G_{N1}(N1-N4)C_{N4}$ ,  $G_{N2}(N2-N3)C_{N4}$ , and  $G_{N2}(N2-N4)C_{N4}$ , see Table 1. The possibility of the formation of G–C cross-link from diradicals is based on the fact that the multiple ionization events are common in radiation damage and guanine and cytosine ionization potentials are such that each would be oxidized once in preference to a double oxidation on a single base. Single-ionization events would lead to G radicals by hole transfer and proton loss, and G radicals could dimerize as well. Thus, we also considered three guanine–guanine N–N cross-linked structures ( $G_{N2}(N2-N2)G_{N2}$ ,  $G_{N2}(N2-N1)G_{N1}$ , and  $G_{N1}(N1-N1)G_{N1}$ ) that can form from reaction between two guanine radicals, see Table 1. The binding energies of all the six G–C diradicals lie in the range of ca. –54 to –68 kcal/mol.  $G_{N1}(N1-N3)C^+$  is the most stable of this group with a binding energy of ca. –68 kcal/mol compared to the isolated  $\cdot G_{N1}$  and  $C^+$ . Figure 2 shows the BHandHLYP/6-31G\*-calculated PES for the reaction of  $\cdot G_{N1}$  and  $C^+$  to form  $G_{N1}(N1-N3)C^+$ . From Figure 2, it is evident that  $\cdot G_{N1}$  and  $C^+$  are very reactive and the formation of  $G_{N1}(N1-N3)C^+$  is highly exothermic and proceeds without a barrier. The plot of the highest occupied molecular orbital (HOMO), shown in Figure 2, for  $G_{N1}(N1-N3)C^+$  in singlet state shows that the HOMO is localized on the guanine moiety and it is the base site for any further oxidation.

At all levels of theory considered in the present study, we found that G–C diradicals are stabilized by strong N–N cross-links and N–N cross-links in singly oxidized G–C systems, shown in Figure 1 and Supporting Information Figure S1, are metastable toward formation of the hydrogen-bonded GC radical. The BHandHLYP/6-31G\*-calculated PESs (Figures S2–S6 in the Supporting Information) for the formation of  $G_{N2}(N2-N3)C^+$ ,  $G_{N1}(N1-N3)C_{N4}$ ,  $G_{N1}(N1-N4)C_{N4}$ ,  $G_{N2}(N2-N3)C_{N4}$ , and  $G_{N2}(N2-N4)C_{N4}$  are similar to the PES for the formation of  $G_{N1}(N1-N3)C^+$  shown in Figure 2.

The bonded G–G diradicals ( $G_{N2}(N2-N2)G_{N2}$ ,  $G_{N2}(N2-N1)G_{N1}$ , and  $G_{N1}(N1-N1)G_{N1}$ ) are also found to be stable with a binding energy in the range of ca. –40 to –47 kcal/mol, but



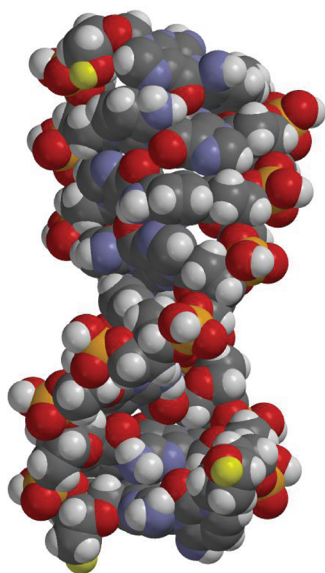
**Figure 2.** BHandHLYP/6-31G\*-calculated potential energy surface (kcal/mol) for the formation of N–N cross-link  $G_{N1}(N1-N3)C^+$  on reaction between  $\cdot G_{N1}$  and  $C^+$  (cytosine cation radical). The spin density distribution in the isolated  $\cdot G_{N1}$  and  $C^+$  and HOMO (highest occupied molecular orbital) in  $G_{N1}(N1-N3)C^+$  are also shown. The net charge and spin (in parentheses in bold) residing in each moiety are also shown. The charge and spin density distribution at each atom of species numbered as I, II, and III are given in Table S3 in the Supporting Information.

interestingly they are substantially less stable than the G–C diradicals, see Table 1.

**IV. Cross-Link Formation between Adenine Radical and Thymine Radical (Diradical).** For adenine–thymine (A–T) diradical only one N–N cross-link structure ( $A_{N6}(N6-N3)T_{N3}$ ) is considered likely. This cross-link is formed by the reaction between  $\cdot A_{N6}$  and  $\cdot T_{N3}$ . The BHandHLYP/6-31G\*-calculated PES for the formation of  $A_{N6}(N6-N3)T_{N3}$  is shown in the Supporting Information as Figure S7. This structure has the substantial binding energy of ca. –80 kcal/mol, and the HOMO is localized on the adenine moiety with some delocalization on thymine.

**V. Cross-Link Formation between T–T and C–C Diradicals.** Hydrogen atom loss from N4 of cytosine and from N3 of thymine result in two radicals, viz.,  $\cdot C_{N4}$  and  $\cdot T_{N3}$ . We considered the homodimers formed by the reaction of  $\cdot T_{N3}$  with  $\cdot T_{N3}$  and  $\cdot C_{N4}$  with  $\cdot C_{N4}$  which give four N–N cross-links, i.e.,  $T_{N3}(N3-N3)T_{N3}$ ,  $C_{N4}(N3-N3)C_{N4}$ ,  $C_{N4}(N3-N4)C_{N4}$ , and  $C_{N4}(N4-N4)C_{N4}$ . The  $T_{N3}(N3-N3)T_{N3}$  cross-link has a binding energy of ca. –98 kcal/mol, whereas the binding energy of the different C–C cross-links lies in the range of ca. –67 to –75 kcal/mol, see Table 1. Among all the homodimers considered,  $T_{N3}(N3-N3)T_{N3}$  is found to be the most stable.

The pyrimidine–pyrimidine N–N cross-links are exceptionally strong, whereas purine homodimers are far weaker with AA more stable than the GG forms. We note that binding in  $T_{N3}(N3-N3)T_{N3}$  is similar in nature to that found for the dimer formed from two succinimide radicals which produces *N*–*N'*-bis-succinimide. This species is thermodynamically quite stable, and the NN bond is found to be resistant to even harsh chemical treatments.<sup>23</sup> This clearly suggests the species described in this work should be quite stable and are expected to be found by experiment.



**Figure 3.** Model of NN-DNA after formation of N–N cross-links between G–C in each base pair in ds 8-mer DNA, 5′-GCGCGCGC-3′, which is  $G_{N1}(N1-N3)C_{N4}$  bonded to its complement, 3′-CGCGCGCG-5′. The structure was modeled in SPARTAN (ref 24) and energy-minimized via the built-in molecular mechanics program. Each phosphate is protonated for charge neutralization.

**VI. Charge and Spin Density Distribution.** The Mulliken charge and spin density located at each atom in the molecule, calculated using the BHandHLYP/6-31G\* method, for the formation of all N–N cross-link structures, considered in this study, are presented in Tables S2–S10 in the Supporting Information. In Figures 1, 2, and Supporting Information Figures S1–S7, the spin partitioning between two moieties forming the N–N cross-link is presented. The analysis of the charge and spin density distributions along the reaction path for the formation of N–N cross-links is important to the understanding of the mechanism of their formation.<sup>24</sup> The formation of  $G_{N1}^{\cdot-}(N1-N3)C^{\cdot+}$ , shown in Figure 1, shows that initially spin density is completely localized on guanine radical and as  $G_{N1}^{\cdot-}$  and C approach each other to form an N1–N3 bond, the spin density transfers from G to C. At the transition state (marked as II in Figure 1), the guanine moiety gains only a little charge ( $-0.093e$ ;  $e$  is the electronic charge) from cytosine, and on the formation of N–N cross-linked structure (marked as I in Figure 1) cytosine gains a very small charge ( $-0.005e$ ). Similar results are also obtained for  $G_{N2}(N2-N3)C^{\cdot+}$  shown in Figure S1 in the Supporting Information. The formation of  $G_{N1}(N1-N3)C^{\cdot+}$  and  $G_{N2}(N2-N3)C^{\cdot+}$  is calculated to be endothermic by 10–15 kcal/mol relative to the separate monomers, see Figure 1 and Supporting Information Figure S1. However, the formation of  $G_{N1}(N1-N3)C^{\cdot+}$  and  $G_{N2}(N2-N3)C^{\cdot+}$  (see Figure 2 and Supporting Information Figure S2), which can be obtained directly by oxidizing  $G_{N1}(N1-N3)C^{\cdot+}$  and  $G_{N2}(N2-N3)C^{\cdot+}$ , are found to be quite stable and have binding energy of ca. 60 kcal/mol. The BHandHLYP/6-31G\*-calculated gas-phase ionization potentials (IP) of  $G_{N1}(N1-N3)C^{\cdot+}$  and  $G_{N2}(N2-N3)C^{\cdot+}$  are 4.83 and 5.08 eV, respectively, and in an aqueous phase, simulated by use of the PCM (polarized continuum model) the corresponding IPs are 3.06 and 2.97 eV, respectively, see Table S11 in the Supporting Information. These ionization potentials

are quite low, and it appears that the unstable cross-links ( $G_{N1}(N1-N3)C^{\cdot+}$  and  $G_{N2}(N2-N3)C^{\cdot+}$ ) can easily be oxidized by electron transfer to existing oxidative species in surrounding proteins or in the DNA stack to form a quite stable species.<sup>25</sup> For N–N cross-linked formed by radical–radical reaction (Table 1 and Supporting Information), charge transfer between two moieties is evident during the interaction, but on bonding only a small charge transfer is found.

**VII. NN-DNA.** On the basis of this work for base pair N–N bonding, a new form of DNA with N–N bonds between G–C base pairs has been modeled. This model of NN-DNA after the formation of N–N cross-links between G–C in each base pair in double-stranded (ds) 8-mer DNA, 5′-GCGCGCGC-3′, is shown in Figure 3. The structure is generated by directly bonding N1 of guanine with N3 of cytosine ( $G_{N1}(N1-N3)C_{N4}$ , see Table 1) in each of the G–C base pairs in the ds 8-mer DNA using the SPARTAN molecular modeling package.<sup>26</sup> The structure is energy-minimized using the molecular mechanics program within the SPARTAN package. In this NN-DNA, each of the base pairs are bonded at ca. 90° between base planes, yet the structure allows for a compact structure. Since each base pair is held together with ca. 60 kcal/mol bond energy (see Table 1) for each of the various G–C NN bond types a robust DNA architecture is created. The integrity of such structures would be expected to be resistant to high temperatures, i.e., no melting would be observed

## CONCLUSION

The interaction of high-LET radiation with DNA stochastically ionizes DNA bases forming radical cations. These species are thermodynamically driven to deprotonate to the surrounding medium to become neutral radicals. These radicals are known to react to form intrastrand cross-link structures some of which have been characterized experimentally.<sup>5,6</sup> This theoretical study investigates the possible formation of N–N cross-linked structures formed from radical–radical reaction between DNA base pairs that have not been considered previously. From the test cases, it is found that the BHandHLYP functional is the most suitable method to treat these hydrazine-like cross-linked structures. The newly developed M06 and M06-2X functionals were found to largely overestimate the G3B3-calculated binding energies in test cases by more than ca. 10 kcal/mol, whereas the BHandHLYP-calculated values had an absolute average deviation of only 3 kcal/mol (average deviation 1 kcal/mol).

The radical–radical (diradical) reaction to form the N–N cross-link is found to be highly exothermic in nature, and  $A_{N6}(N6-N3)T_{N3}$  cross-link among the base pair cross-links has the largest binding energy (ca.  $-80$  kcal/mol, BHandHLYP), whereas GC cross-linked structures have binding energies that range from  $-54$  to  $-69$  kcal/mol. The HOMO in all the base-paired N–N cross-link structures is found to be localized mainly on the purine (G and A) moiety, and the LUMO is on the pyrimidine (T and C). The possibility of reaction between G radical and neutral C to form N–N cross-linked radical was also considered; however, it is endothermic in nature by ca. 10 kcal/mol forming a metastable intermediate which transferred the spin from G to C. This species is found to have a low ionization energy and would readily be oxidized to the more strongly bonded N–N cross-linked structure. When N–N radical–radical cross-links between the same base are considered, i.e., GG, AA, CC, and TT, it is clear that the pyrimidines are far stronger than the purine NN cross-links. Most surprising was the



98 kcal/mol cross-link in  $T_{N_3}(N_3-N_3)T_{N_3}$ , which will be treated in more detail in a subsequent publication.

Our work clearly shows that a number of the DNA base N–N cross-linked structures, considered in this work, are predicted to be more stable than hydrazine (64 kcal/mol) and therefore sufficiently thermodynamically stable to isolate them from irradiated DNA systems. We encourage experimental laboratories to seek such dimers formed from N–N bonding of base radicals in DNA systems.

## ■ ASSOCIATED CONTENT

**S Supporting Information.** Tables of binding energies, charge and spin density distributions of different N–N cross-links computed using different DFT methods, and BHand-HLYP/6-31G\*-computed potential energy surfaces (PESs) for the formation of different N–N cross-link structures. This material is available free of charge via the Internet at <http://pubs.acs.org>.

## ■ ACKNOWLEDGMENT

This work was supported by the NIH NCI under Grant No. R01CA045424, and computational studies were supported by a computational facilities Grant, NSF CHE-0722689. We thank Professor Robert Anderson, Department of Chemistry, The University of Auckland and Professor Arthur Bull, Department of Chemistry, Oakland University for helpful discussions.

## ■ REFERENCES

- (1) (a) Becker, D.; Sevilla, M. D. Radiation damage to DNA related biomolecules. In *Royal Society of Chemistry Specialist Periodical Report. Electron Spin Resonance*; Gilbert, B. C.; Davies, M. J.; Murphy, D. M., Eds.; Royal Society of Chemistry: Cambridge, U.K., 2008; Vol. 21, pp 33–56. (b) Kumar, A.; Sevilla, M. D. Theoretical modeling of radiation-induced DNA damage. In *Radical and Radical Ion Reactivity in Nucleic Acid Chemistry*; Greenberg, M. M., Ed.; John Wiley & Sons, Inc.: Hoboken, NJ, 2009; pp 1–40. (c) Kumar, A.; Sevilla, M. D. Radiation effects on DNA: Theoretical investigations of electron, hole and excitation pathways to DNA damage. In *Radiation Induced Molecular Phenomena in Nucleic Acid: A Comprehensive Theoretical and Experimental Analysis*; Shukla, M. K.; Leszczynski, J., Eds.; Springer-Verlag: Heidelberg, Germany, 2008; pp 577–617. (d) Bernhard, W. A. Radical reaction pathways initiated by direct energy deposition in DNA by ionizing radiation. In *Radical and Radical Ion Reactivity in Nucleic Acid Chemistry*; Greenberg, M. M., Ed.; John Wiley & Sons, Inc.: Hoboken, NJ, 2009; pp 41–68. (e) Becker, D.; Adhikary, A.; Sevilla, M. D. Physicochemical mechanisms of radiation induced DNA damage. In *Charged Particle and Photon Interactions with Matter—Recent Advances, Applications, and Interfaces*; Hatano, Y.; Katsumura, Y.; Mozumder, A., Eds.; CRC Press, Taylor and Francis Group: Boca Raton, FL, 2010; pp 503–541. (f) Kumar, A.; Sevilla, M. D. *Chem. Rev.* **2010**, *110*, 7002–7023.
- (2) Pimblott, S. M.; Mozumder, A. J. *Phys. Chem.* **1991**, *95*, 7291–7300.
- (3) LaVerne, J. A.; Pimblott, S. M. *Radiat. Res.* **1995**, *141*, 208–215.
- (4) (a) Becker, D.; Bryant-Friedrich, A.; Trzasko, C.; Sevilla, M. D. *Radiat. Res.* **2003**, *160*, 174–185. (b) Becker, D.; Razzkazovskii, Y.; Callaghan, M. U.; Sevilla, M. D. *Radiat. Res.* **1996**, *146*, 361–368.
- (5) (a) deLara, C. M.; Jenner, T. J.; Townsend, K. M. S.; Marsden, S. J.; O'Neill, P. *Radiat. Res.* **1995**, *144*, 43–49. (b) Münzel, M.; Szeibert, C.; Glas, A. F.; Globisch, D.; Carell, T. *J. Am. Chem. Soc.* **2011**, *133*, 5186–5189 and references therein. (c) Box, H. C.; Dawidzik, J. B.; Budzinski, E. E. *Free Radical Biol. Med.* **2001**, *31*, 856–868.
- (6) (a) Greenberg, M. M. Pyrimidine Nucleobase Radical Reactivity. In *Radical and Radical Ion Reactivity in Nucleic Acid Chemistry*; Greenberg, M. M., Ed.; John Wiley & Sons, Inc.: Hoboken, NJ, 2009; pp 135–162 and references therein. (b) Shapiro, R.; Dubelman, S.; Feinberg, A. M.; Crain, P. F.; McCloskey, J. A. *J. Am. Chem. Soc.* **1977**, *99*, 302–303. (c) Dubelman, S.; Shapiro, R. *Nucleic Acids Res.* **1977**, *4*, 1815–1828. (d) Kirchner, J. J.; Hopkins, P. B. *J. Am. Chem. Soc.* **1991**, *113*, 4681–4682. (e) Kirchner, J. J.; Sigurdsson, S. T.; Hopkins, P. B. *J. Am. Chem. Soc.* **1992**, *114*, 4021–4027. (f) Harwood, E. A.; Hopkins, P. B.; Sigurdsson, S. T. *J. Org. Chem.* **2000**, *65*, 2959–2964. (g) Harwood, E. A.; Sigurdsson, S. T.; Edfeldt, N. B. F.; Reid, B. R.; Hopkins, P. B. *J. Am. Chem. Soc.* **1999**, *121*, 5081–5082. (h) Riccardis, F. D.; Johnson, F. *Org. Lett.* **2000**, *2*, 293–295. (i) Glaser, R.; Wu, H.; Lewis, M. *J. Am. Chem. Soc.* **2005**, *127*, 7346–7358. (j) Roos, W. P.; Tsaalbi-Shtylik, A.; Tsaryk, R.; Güvercin, F.; de Wind, N.; Kaina, B. *Mol. Pharmacol.* **2009**, *76*, 927–934. (k) Fischhaber, P. L.; Gall, A. S.; Duncan, J. A.; Hopkins, P. B. *Cancer Res.* **1999**, *59*, 4363–4368. (l) Xerri, B.; Morell, C.; Grand, A.; Cadet, J.; Cimino, P.; Barone, V. *Org. Biomol. Chem.* **2006**, *4*, 3986–3992. (m) Humphreys, W. G.; Kadlubar, F. F.; Guengerich, F. P. *Proc. Natl. Acad. Sci. U.S.A.* **1992**, *89*, 8278–8282.
- (7) Hawley, R. C.; Kiessling, L. L.; Schreiber, S. L. *Proc. Natl. Acad. Sci. U.S.A.* **1989**, *86*, 1105–1109.
- (8) (a) Bergene, R.; Melo, T. B. *Int. J. Radiat. Biol.* **1973**, *23*, 263–270. (b) Dulcic, A.; Herak, J. N. *Radiat. Res.* **1971**, *47*, 573–580. (c) Dulcic, A.; Herak, J. N. *Biochim. Biophys. Acta* **1973**, *319*, 109–115.
- (9) Peoples, A. R.; Mercer, K. R.; Bernhard, W. A. *J. Phys. Chem. B* **2010**, *114*, 9283–9288.
- (10) Adhikary, A.; Kumar, A.; Munafo, S. A.; Khanduri, D.; Sevilla, M. D. *Phys. Chem. Chem. Phys.* **2010**, *12*, 5353–5368.
- (11) (a) Bera, P. P.; Schaefer, H. F. *Proc. Natl. Acad. Sci. U.S.A.* **2005**, *102*, 6698–6703. (b) Lind, M. C.; Bera, P. P.; Richardson, N. A.; Wheeler, S. E.; Schaefer, H. F. *Proc. Natl. Acad. Sci. U.S.A.* **2006**, *103*, 7554–7559. (c) Evangelista, F. A.; Paul, A.; Schaefer, H. F. *J. Phys. Chem. A* **2004**, *108*, 3565–3571. (d) Evangelista, F. A.; Schaefer, H. F. *J. Phys. Chem. A* **2004**, *108*, 10258–10269. (e) Profeta, L. T. M.; Larkin, J. D.; Schaefer, H. F. *Mol. Phys.* **2003**, *101*, 3277–3284. (f) Luo, Q.; Li, J.; Li, Q. S.; Kim, S.; Wheeler, S. E.; Xie, Y. M.; Schaefer, H. F. *Phys. Chem. Chem. Phys.* **2005**, *7*, 861–865.
- (12) Seal, P.; Jha, P. C.; Agren, H.; Chakrabarti, S. *Chem. Phys. Lett.* **2008**, *465*, 285–289.
- (13) Frisch, M. J.; et al. Gaussian 09; Gaussian, Inc.: Wallingford, CT, 2009.
- (14) GaussView; Gaussian, Inc.: Pittsburgh, PA, 2003.
- (15) Jmol: An open-source Java Viewer for chemical structures in 3D; Jmol Development Team, An Open-Science Project, 2004; available at <http://jmol.sourceforge.net>.
- (16) Neese, F.; Hansen, A.; Wennmohs, F.; Grimme, S. *Acc. Chem. Res.* **2009**, *42*, 641–648.
- (17) (a) Guidon, M.; Hutter, J.; VandeVondele, J. *J. Chem. Theory Comput.* **2010**, *6*, 2348–2364. (b) Korth, M.; Grimme, S. *J. Chem. Theory Comput.* **2009**, *5*, 993–1003. (c) Goerigk, L.; Grimme, S. *J. Chem. Theory Comput.* **2011**, *7*, 291–309. (d) Henderson, T. M.; Izmaylov, A. F.; Scalmani, G.; Scuseria, G. E. *J. Chem. Phys.* **2009**, *131*, 044108-1–044108-9. (e) Kumar, A.; Sevilla, M. D. *J. Phys. Chem. B* **2011**, *115*, 4990–5000.
- (18) Baboul, A. G.; Curtiss, L. A.; Redfern, P. C.; Raghavachari, K. *J. Chem. Phys.* **1999**, *110*, 7650–7657.
- (19) (a) Wiberg, K. B. *J. Phys. Chem.* **1992**, *96*, 5800–5803. (b) Jursic, B. S. *J. Mol. Struct. (THEOCHEM)* **1996**, *366*, 103–108.
- (20) Steenken, S. *Chem. Rev.* **1989**, *89*, 503–520.
- (21) (a) Adhikary, A.; Kumar, A.; Becker, D.; Sevilla, M. D. *J. Phys. Chem. B* **2006**, *110*, 24171–24180. (b) Anderson, R. F.; Shinde, S. S.; Maroz, A. *J. Am. Chem. Soc.* **2006**, *128*, 15966–15967. (c) Kobayashi, K.; Tagawa, S. *J. Am. Chem. Soc.* **2003**, *125*, 10213–10218. (d) Chatgililoglu, C.; Caminal, C.; Guerra, M.; Mulazzani, Q. G. *Angew. Chem., Int. Ed.* **2005**, *44*, 6030–6032. (e) Adhikary, A.; Khanduri, D.; Sevilla, M. D. *J. Am. Chem. Soc.* **2009**, *131*, 8614–8619. (f) Kumar, A.; Sevilla, M. D. *J. Phys. Chem. B* **2009**, *113*, 11359–11361.
- (22) (a) Steenken, S.; Reynisson, J. *Phys. Chem. Chem. Phys.* **2010**, *12*, 9088–9093. (b) Reynisson, J.; Steenken, S. *Phys. Chem. Chem. Phys.* **2002**, *4*, 5346–5352.

- (23) (a) Hedaya, E.; Hinman, R. L.; Schomaker, V.; Theodoropoulos, S.; Kyle, L. M. *J. Am. Chem. Soc.* **1967**, 89, 4875–4884. (b) Hedaya, E.; Hinman, R. L.; Theodoropoulos, S. *J. Org. Chem.* **1966**, 31, 1311–1316. (c) Hedaya, E.; Hinman, R. L.; Theodoropoulos, S. *J. Org. Chem.* **1966**, 31, 1317–1326. (d) Coleman, D. J.; Skinner, H. A. *Trans. Faraday Soc.* **1966**, 62, 2057–2062.
- (24) Mitrasinovic, P. M. *Bioconjugate Chem.* **2005**, 16, 588–597.
- (25) Prütz, W. A.; Butler, J.; Land, E. J.; Swallow, A. J. *Biochem. Biophys. Res. Commun.* **1980**, 96, 408–414.
- (26) SPARTAN, version 10; Wavefunction, Inc.: Irvine, CA, 1997.